phys. stat. sol. (a) **205**, No. 11, 2560–2565 (2008) / **DOI** 10.1002/pssa.200880222

physica status solidi a
www.pss-a.com
applications and materials science

Growth of III-nitride quantum dots and their applications to blue-green LEDs

T. D. Moustakas*[1], Tao Xu[1], C. Thomidis[1], A. Yu Nikiforov[1], Lin Zhou[2], and David J. Smith[2]

[1] Department of Electrical and Computer Engineering, and Center for Photonics Research, Boston University, Boston MA 02215, USA
[2] School of Materials and Department of Physics, Arizona State University, Tempe, Arizona 85287, USA

Received 17 January 2008, revised 20 May 2008, accepted 25 May 2008
Published online 18 September 2008

PACS 81.07.Ta, 81.15.Hi, 85.35.Be, 85.60.Jb

* Corresponding author: e-mail moustakas@bu.edu, Phone: +10 617 353 5431, Fax: +10 617 353 6440

In this paper we discuss the growth of InN, GaN and InGaN QDs by MBE on either GaN or AlN templates. InN QDs on GaN templates were found to occur without an InN wetting layer, a result consistent with the large lattice mismatch of 11% between InN and GaN. Self-assembled GaN QDs were grown on AlN templates, using the modified Stranski-Krastanov mode of growth. The microstructure and the size distribution of such QDs in a single layer or a superlattice structure were investigated by electron microscopy and atomic force microscopy. Finally, the self assembly of InGaN QDs on GaN templates using the Stranski-Krastanov mode and the applications of such QDs to blue-green LEDs are addressed. The results indicate that InGaN / GaN multiple quantum dots (MQDs) are highly strained and their emission at low injection is red shifted with respect to that of a single layer of QDs due to quantum confined Stark effect.

© 2008 WILEY-VCH Verlag GmbH & Co. KGaA, Weinheim

1 Introduction LEDs emitting in the violet-blue-green parts of the electromagnetic spectrum are based on InGaN multiple quantum wells (MQWs). The internal quantum efficiency (IQE) of such devices decreases as the InN mole fraction in the InGaN wells increases, a result that has not been fully understood. Alloy phenomena and/or strong piezoelectric fields across the QWs could possibly contribute to this decrease in IQE.

Alloy phenomena such as spinodal decomposition driven phase separation [1, 2] lead to compositional inhomogeneities and the resulting potential fluctuations have been thought to be beneficial to emission by LEDs due to localization of excitons [3]. However, III-Nitride alloys were also found to undergo partial atomic ordering [4-6], and this was thought to be undesirable to LED performance, because electron-hole pairs tend to separate in the ordered and random domains and this minimizes the efficiency of spontaneous radiative recombination [7]. Theoretical calculations by Dudiy and Zunger [8] on partially ordered $Al_xGa_{1-x}N$ indicate that the energy band alignment between random and ordered domains changes from Type I to Type II heterostructures for x ~ 0.4. This leads to an increase by two to three orders of magnitude in the radiative lifetimes of injected e-h pairs. Although such studies have not been reported in InGaN alloys one expects qualitatively a similar behaviour. Thus, the spontaneous radiative lifetime is expected to increase with the increase in InN mole fraction.

The role of the piezoelectric fields across the QWs in influencing the performance of InGaN LEDs has also been addressed by a number of authors [9, 10]. In particular, since the strength of the piezoelectric fields across the InGaN QWs increases as the InN mole fraction increases.

An alternative approach is to use InGaN quantum dots (QDs) instead of QWs as the active region of the LED. In such LED structures exciton localization occurs by 3D quantum confinement rather than by potential fluctuations due to compositional inhomogeneities. This is because the density of states of QDs has delta-function energy dependence. Of course electron confinement in all three dimensions requires that the lateral dimensions of the QDs are equal or smaller than the de Broglie wavelength of electrons. In such small structures phase separation and partial atomic ordering are not likely to occur. However, piezoelectric fields are likely to be as important in the case of QDs as in QWs. For this reason the QDs must be 1 to 2 nm

WILEY InterScience DISCOVER SOMETHING GREAT

© 2008 WILEY-VCH Verlag GmbH & Co. KGaA, Weinheim

in average size to minimize the quantum confined Stark effect (QCSE).

In this paper we review our progress in the fabrication and characterization of III-Nitride QDs and their application to blue-green LEDs. In particular we discuss the problems with the current generation QDs and what improvements in the growth and microstructure are required to lead to more efficient LEDs than those based on quantum wells.

2 Experimental methods The InN, GaN and InGaN QDs were grown by rf plasma-assisted MBE using the Varian Gen II MBE system. Ga, Al and In were evaporated from standard effusion cells and the molecular nitrogen was activated in an EPI rf plasma source. The plasma power was kept at 300 W and the nitrogen flow rate was 1.0 sccm. In all cases c-plane sapphire substrates were used, which led to InN, GaN and InGaN QDs having the [0001] orientation. The sapphire substrates were first subjected to nitridation at 870 °C for approximately 1 h, followed by the deposition of a 60-300-nm thick AlN film grown at the same temperature under Al-rich conditions of growth. These nucleation steps lead to group-III polar growth on c-sapphire substrates. The specific growth conditions of the three types of QDs investigated are described in Section 3.

The surface dot density and height distribution were evaluated using Atomic Force Microscopy (AFM). The structure and microstructure of the dots was determined by transmission electron microscopy (TEM). Observations were made in both plan-view and cross-section geometries with a JEM-4000EX high-resolution electron microscope.

3 Results and discussion In this section we discuss the growth and characterization of InN, GaN and InGaN QDs as well as our initial efforts to incorporate such QDs in blue –green LEDs.

3.1 InN quantum dots Details on the growth and structure of InN QDs were published elsewhere [11] and in here we only review the most important findings. Following the deposition of 60 nm AlN as described in the previous section, a 500-nm thick Ga-polar GaN film was grown at 770 ˚C under slightly Ga-rich conditions. Standard **g.b** diffraction contrast analysis revealed that dislocations of either edge or mixed (edge-screw) type were the primary threading defects present in this relatively thin GaN buffer layer. Plan-view observations revealed that the dislocation densities were typically in the range of $2\text{-}5\times10^{10}/\text{cm}^2$. The InN QDs were deposited at substrate temperature of 425 ˚C. The relatively low temperature was chosen primarily because of the low decomposition temperature of In-polar InN. The typical equivalent growth rate for InN deposition was ~0.05 nm/s. A total equivalent coverage of approximately nine InN monolayers [where one monolayer (ML) ~0.285 nm] was used during the deposition of the InN QDs. The sample was annealed for 5 min at the growth temperature under N-atmosphere before cooling down.

Figure 1 shows a typical panorama showing the apparently random distribution of the InN QDs. From these data we calculated the quantum dot density to be $\sim 2\times10^9/\text{cm}^2$ and the mean diameter and height dimensions were 115 and 15 nm respectively.

Both *in-situ* reflection high energy electron diffraction (RHEED) and *ex-situ* transmission electron microscopy show no evidence of InN wetting layer, a result consistent with the large lattice mismatch (11%) between GaN and InN. Examination by electron microscopy indicates that almost all of the InN islands have nucleated directly above threading dislocations present in the GaN buffer. Detailed examination at higher magnifications indicates that the InN QDs have the wurtzite crystal structure and that the QDs also maintained a well defined epitaxial relationship with the underlying GaN buffer layer. Periodic arrays of moiré fringes with spacings of ~ 2.8 nm were visible along the InN QD/ GaN buffer layer interface, as would be expected for perfect InN/GaN heteroepitaxy. This periodicity also corresponds to the spacings between the misfit dislocations that would accommodate the lattice mismatch between the two materials. This is an indication that the InN QDs are completely relaxed.

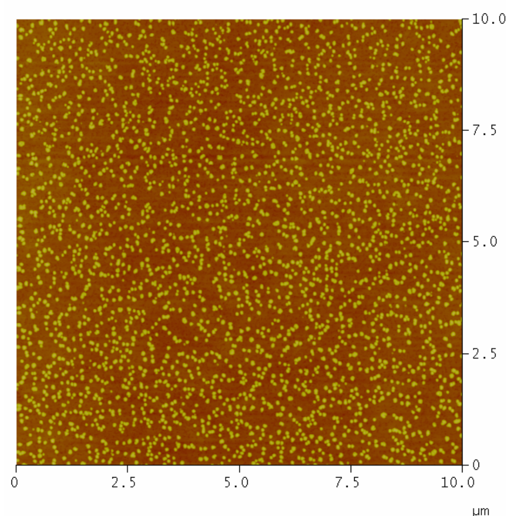

Figure 1 AFM image showing distribution of InN QDs grown on a Ga-polar GaN template.

3.2 GaN quantum dots Details on the growth and characterization of GaN QDs were published elsewhere [12] and in here we summarize the most important findings. After the deposition of 300 nm AlN on the substrate at 870 °C the substrate temperature was then reduced to 770 °C for the deposition of GaN QDs or QD superlattice consisting of GaN QDs separated by 10-20 nm AlN barriers. The growth rate of the GaN QDs was about 0.3 ML/s. The GaN QDs were grown in the modified Stranski-Krastanov growth mode [13, 14]. In this mode several MLs of GaN were deposited under Ga-rich conditions (Ga/N ~

© 2008 WILEY-VCH Verlag GmbH & Co. KGaA, Weinheim

1.1), followed by evaporation of the excess Ga in vacuum. During this stage the deposited GaN film undergoes 2D to 3D transition as indicated by the conversion of the RHEED pattern from streaky to spotty.

Figure 2 shows a high resolution TEM image of two GaN QDs at the last layer of a QD superlattice, consisting of four periods of GaN/AlN. The GaN QDs were obtained using 5 ML of GaN coverage, and the QDs are separated by 18 nm AlN barriers. From this electron micrograph we estimate that the height of the QDs is about 4 nm and that the dot diameter is about 15 nm. The QDs in the free surface have truncated pyramidal shapes, faceted along the {1-103} planes. A continuous 2D wetting layer with a thickness of about 2-2.5 ML was identified from these studies. These findings agree with other published results [15].

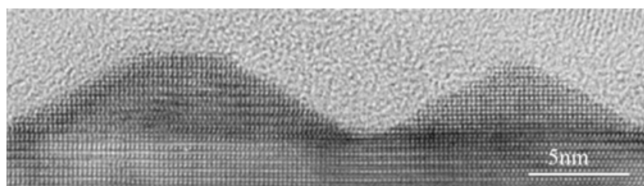

Figure 2 High resolution TEM image of GaN QDs on the surface of a 4 period GaN/AlN QD superlattice.

The surface morphology of this GaN quantum dot superlattice (QDSL) is shown in the AFM image of Fig. 3. The QD density on the top surface of this QD superlattice was measured to be $9x10^{10}$ cm^{-2}.

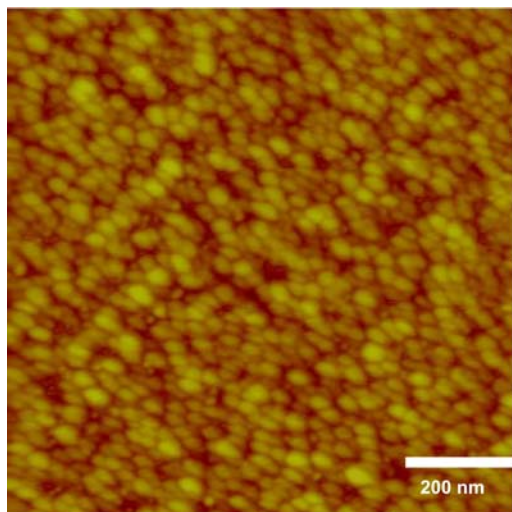

Figure 3 AFM height image of a GaN QDSL with four stacks of QDs and 5 ML GaN coverage in each stack (z scale is 10 nm).

The height distribution of the surface GaN QDs for samples produced with different GaN coverage are shown in Fig. 4. Thus, the height of the GaN QDs has a bimodal distribution. Mode 1 has a narrow Gaussian distribution with an average height of 1.4-1.8 nm and full width at half maximum of 0.8 to 0.9 nm. Mode 2 has a broader distribution with an average height of about 3.6 nm and FWHM of 2 nm. As the GaN coverage increases, mode 2 becomes the dominant one. When the coverage is more than 5 ML, the height distribution becomes practically Gaussian with an average height of about 3.4 nm and FWHM of 1.8-1.9 nm. The height of mode 2 dots did not increase with increasing coverage, which was different from that reported for GaN QDs grown under N-rich conditions [16].

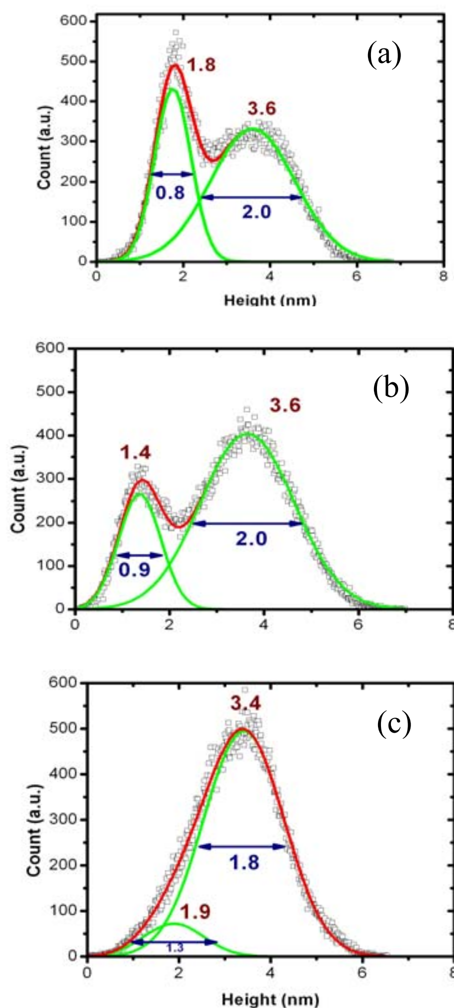

Figure 4 AFM height distribution for GaN QDs grown with (a) 3, (b) 4, and (c) 5 ML GaN coverage, respectively.

Bright-field plan-view TEM images were used to determine the density of dislocations with edge components as well as to access any correlation between dislocations and QDs. Figure 5 shows an image of the GaN QDSL sample with 30 GaN stacks. The patches of faint dark contrast correspond to the GaN QDs, while the small dark

© 2008 WILEY-VCH Verlag GmbH & Co. KGaA, Weinheim

spots correspond to dislocations having edge components. As shown in this image, some GaN QDs are associated with threading dislocations while other QDs appear to be located in areas that are free of dislocations. Moreover, the GaN QDs associated with dislocations sometimes appear to have a larger diameter than QDs in dislocation free regions. These results are in agreement with previous reports [17].

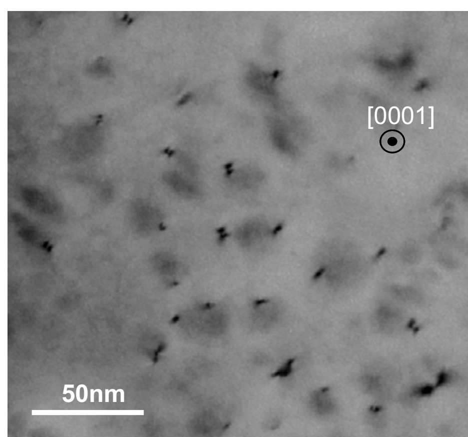

Figure 5 Bright-field plan-view TEM image of GaN QDSL sample with 30 GaN stacks.

To further investigate the origin of the bimodal distribution we have also studied the GaN QD height distribution as a function of the periods of the QDSL. The height distribution for the QDs on the top layer of three GaN/AlN QDSL samples with 1, 4 and 30 stacks is shown in Fig. 6. Again, the height of the GaN QDs has a bimodal distribution. However, mode 1 becomes the dominant one as the number of stacks increases. In fact the density of mode 1 QDs remains the same while the mode 2 QDs decreases with the number of stacks. This result is also consistent with the association of the larger QDs with threading dislocations since it is known that threading dislocations annihilate as the number of stacks increases [12].

This bimodal height distribution of GaN QDs grown heteroepitaxially on highly dislocated nitride templates is undesirable for the use of GaN QDs in a number of applications.

3.3 InGaN quantum dots The InGaN QDs were grown at 520 to 580 °C on 500 nm Ga-polar MBE grown GaN templates. The self-assembled InGaN QDs were grown in the Stranski-Krastanov growth mode. In this mode, several MLs of InGaN were deposited under N-rich conditions. After the thickness of the deposited InGaN exceeds the critical thickness we have observed the 2D to 3D transition by RHEED. At that stage the QD layer was left in vacuum for 1 min before the sample was cooled to room temperature. The dependence of the size distribution and emission properties of these InGaN QDs were reported previously [18]. Figure 7 shows a typical AFM image of an InGaN QD sample grown at 520 °C with equal fluxes of Ga and In and 12 ML InGaN coverage. The average dot height and diameter are 3 nm and 30 nm respectively and the dot density is $7x10^{10}$ cm^{-2}.

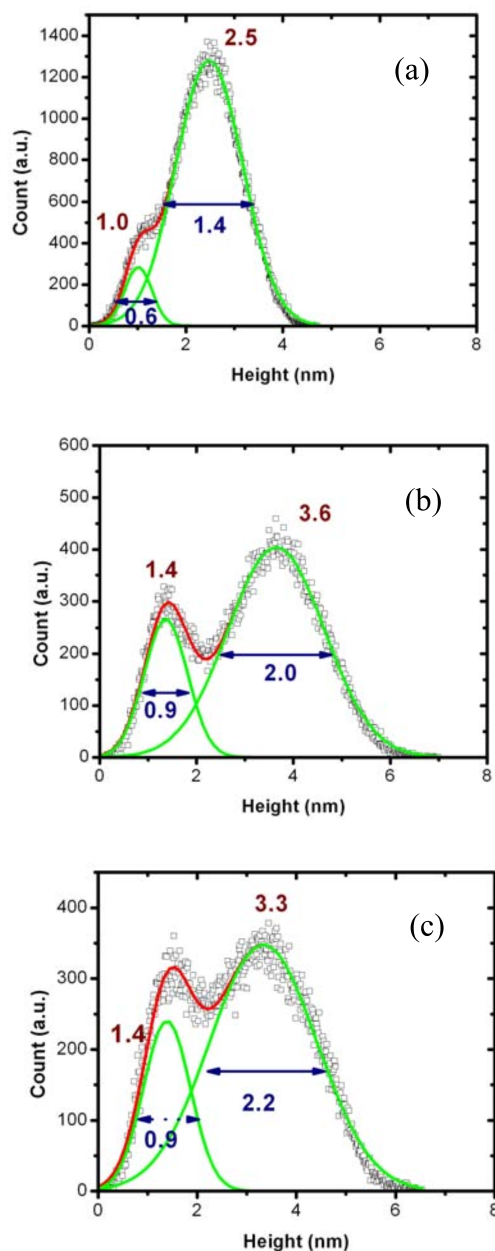

Figure 6 Height distribution of GaN/AlN QDSL samples for different number of stacks and the same GaN coverage (4 ML) in each stack. (a) 1 stack, (b) 4 stacks, and (c) 30 stacks [12].

In addition to single InGaN QDs we have also deposited InGaN/ GaN multiple quantum dots (MQDs) at the same temperature. It contains ten stacks of InGaN QDs, each layer with 12 ML InGaN coverage.

© 2008 WILEY-VCH Verlag GmbH & Co. KGaA, Weinheim

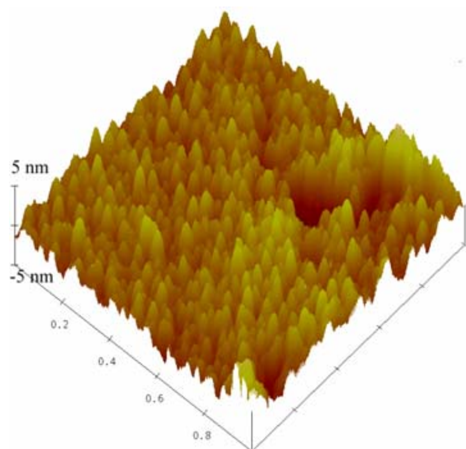

Figure 7 AFM image of an InGaN QD sample grown under the conditions described in the text.

The composition and thicknesses of the InGaN QDs and GaN barriers were determined by XRD to be 43% InN mole fraction and 4 and 6 nm respectively. The emission properties of these InGaN QDs and MQDs were investigated by cathodoluminescence measurements at room temperature. Specifically, the single InGaN QDs were investigated at 3 kV accelerating voltage, while the InGaN/GaN MQDs were investigated at 13 kV accelerating voltage. The results are shown in Fig. 8.

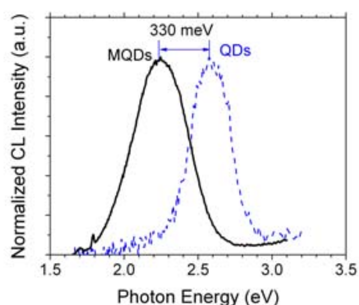

Figure 8 Room temperature CL emission of a single layer of InGaN QDs (blue) and an InGaN/GaN MQD sample with identical InGaN QDs [17].

We note that the emission spectra from the single layer of InGaN QDs have its peak at 2.58 eV and a FWHM of 308 meV, while that of the MQD have a peak at 2.25 eV and FWHM of 415 meV. Thus, the spectra of the MQDs have been red shifted by 330 meV and broadened by 107 meV. The relatively broad emission spectra suggest a rather broad size distribution of InGaN QDs. We speculate that the significant red shift of the emission spectra of the MQDs is consistent with strong QCSE since the InGaN QDs in the MQD structure are subjected to greater strain from the GaN barriers. We came to this conclusion since the dots in successive layers are spatially correlated [12]. In other words the QDs in the new layer tend to nucleate directly above the buried QDs. This spatial bias is attributed to the strain in the surface of the new barrier due to the buried strained QDs [19-23]. Indeed, Gogneau et al. reported that in GaN /AlN QD superlattices both the in plain strain of the AlN barriers as well as the elastic relaxation of the GaN QDs depend on the number of stacks [24].

3.4 Blue-green LEDs based on nitride QDs Two types of LED structures employing III-Nitride QDs, designed to emit in the blue and green, were grown and characterized in bare die configuration. Both structures were designed to have GaN QDs in the nucleation layer, which was shown to filter threading dislocations [25]. The blue LED has an active region consisting of 3 $In_{0.18}Ga_{0.82}N$/GaN MQWs. The active regions of the green LED is made of 5 periods of InGaN/GaN MQDs with the InGaN composition of 41%. The InGaN QD layer height and barrier thickness are 4 nm and 6 nm respectively. A schematic of the cross-section structure of the two LEDs is shown in Fig. 9 (upper panel) and photographs of the two devices upon injection with 50 mA current are shown in Fig. 9 (lower panel).

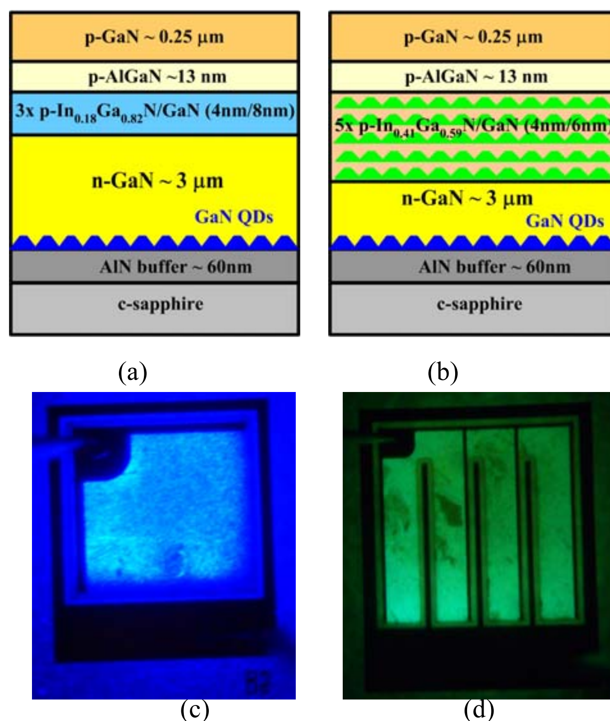

Figure 9 (Upper panel) Schematic of two LED structures grown with GaN QDs in the nucleation layer. (a) Employs 3 InGaN/GaN QWs as the active region and (b) Employs 5 stacks of InGaN QDs as the active region. (Lower panel) Photographs of the two prototype LEDs upon injection with 50 mA are shown in (c) and (d) respectively. The dimensions of the devices are 800 µm x800 µm.

At low injection current the peak emission from the blue LED occurs at 440 nm while that of the green LED occurs at 560 nm. In both of these devices the emission

© 2008 WILEY-VCH Verlag GmbH & Co. KGaA, Weinheim

spectra are blue shifted with increase in the injection current. However, the blue shift is even stronger for the green LED due to the stronger QCSE resulting from the relative large size of the QDs.

4 Conclusions Self-assembled InN, GaN and InGaN QDs and QD superlattices were grown by MBE using different variants of the Stranski-Krastanov growth mode. The InN QDs were grown on Ga-polar GaN templates at 425 °C without a wetting layer and they are fully relaxed. The GaN QDs were grown on an AlN buffer at 770 °C with a wetting layer approximately 2 ML thick. These GaN QDs were found to have a bimodal height distribution. The larger dots nucleate adjacent to dislocations, while the smaller ones nucleate in regions free of dislocations. Both types of QDs have a Gaussian height distribution and mode 2 (larger dots) dominate as the GaN coverage increases. These findings are in general agreement with other reports in the literature on GaN QDs [13-17, 24]. The InGaN QDs were grown on Ga-polar GaN templates at 520 °C. The emission spectra of both a single layer of InGaN QDs as well as InGaN QDs/ GaN superlattices are relatively broad indicating broad size distribution of QDs. The emission spectra of MQDs are red shifted with respect to the spectra from the single layer of QDs, a result attributed to QCSE. Prototype LEDs employing GaN QDs in the nucleation region to filter threading dislocations have been grown and evaluated. LEDs having InGaN QDs with 40% InN mole fraction in the active region were found to emit in the green (560 nm) at low injection current. However, significant blue shift of the EL spectra was observed under high injection a result consistent with strong CQSE due to relatively large size of the InGaN QDs. Based on these preliminary data, the growth of better green LEDs based on InGaN QDS will require the growth of single mode height distribution and small average dimension of InGaN QDs. We propose that this can be accomplished by using low dislocation density GaN templates and low InGaN coverage during their growth.

Acknowledgements This work was partially supported by the Department of Energy (DE-FC26-04NT42275) and the UNLV Research Foundation.

References

[1] I. Ho and G. B. Stringfellow, Appl. Phys. Lett. **69**, 2701 (1996).
[2] R. Singh, D. Doppalapudi, T. D. Moustakas, and L.T. Romano, Appl. Phys. Lett. **70**, 1089 (1997).
[3] S. F. Chichibu, T. Azuhata, T. Sota, and S. Nakamura, Appl. Phys. Lett. **70**, 2822 (1997).
[4] D. Korakakis K. F. Ludwig, and T. D. Moustakas, Appl. Phys. Lett. **71**, 72 (1997).
[5] D. Doppalapudi, S.N. Basu, K.F. Ludwig, and T. D. Moustakas, J. Appl. Phys. **84**, 1389 (1998).
[6] D. Doppalapudi, S.N. Basu and T.D. Moustakas. J. Appl. Phys. **85**, 883 (1999).
[7] M. Misra, D. Korakakis, H. M. Ng, and T.D. Moustakas, Appl. Phys. Lett. **74**, 2203 (1999).
[8] S. V. Dudiy and A. Zunger, Appl. Phys. Lett. **84**, 1874 (2004).
[9] A. Bell, J. Christen, F. Bertram, F. A. Ponce, H. Marui, and S. Tanaka, Appl. Phys. Lett. **84**, 58 (2004).
[10] I. H. Brown, I. A. Pope, P. M. Smowton, J. D. Thomson, W. W. Chow, and D. P. Bour, Appl. Phys. Lett. **86**, 131108 (2005).
[11] L. Zhou, Tao Xu, D. J. Smith, and T. D. Moustakas, Appl. Phys. Lett. **88**, 231906 (2006).
[12] Tao Xu, Lin Zhou, Yiyi Wang, Ahmet S. Ozcan, K. F. Ludwig, D. Smith, and T. D. Moustakas, J. Appl. Phys. **102**, 073517 (2007).
[13] N. Gogneau, D. Jalabert, E. Monroy, T. Tanaka, and B. Daudin, J. Appl. Phys. **94**, 2254 (2003).
[14] J. Brown, F. Wu, P. M. Petroff, and J.S. Speck, Appl. Phys. Lett. **84**, 690 (2004).
[15] E. Sterigiannidou, E. Monroy, B. Daudin, J. L. Rouviere, and A. D. Andreev, Appl. Phys. Lett. **87**, 203112 (2005).
[16] C. Adelmann, B. Daudin, R. A. Oliver, G.A. D. Briggs, and R. E. Rudd, Phys. Rev. B **70**, 125427 (2004).
[17] J. L. Rouviere, J. Simon, N. Pelekanos, B. Daudin, and G. Feuillet, Appl. Phys. Lett. **75**, 2632 (1999).
[18] Tao Xu, A. Nikiforov, R. France, C. Thomidis, A. Williams, and T. D. Moustakas, phys. stat. sol. (a) **204**(6), 2098 (2007).
[19] D. J. Eaglsham and M. Cerullo, Phys. Rev. Lett. **64**, 1943 (1990).
[20] F. K. LeGoues, M. Copel, and R. M. Tromp, Phys. Rev. Lett. **63**, 1826 (1989)
[21] T. S. Kuan and S.S. Iyer, Appl. Phys. Lett. **59**, 2242 (1991).
[22] J. Y. Yao, T. G. Anderson, and G.L. Dunlop, J. Appl. Phys. **69**, 2224 (1991).
[23] J. Tersoff, C. Teichert, and M. G. Lagally, Phys. Rev. Lett. **76**, 1675 (1996).
[24] N. Gogneau, F. Fossard, E. Monroy, S. Monnoye, H. Mank, and B. Daudin, Appl. Phys. Lett. **84**, 4224 (2004).
[25] Tao Xu, A. Yu Nikiforov, C. Thomidis, R. France, A. Williams, W. Li, T. D. Moustakas, L. Zhou, and D. J. Smith (to be published).

© 2008 WILEY-VCH Verlag GmbH & Co. KGaA, Weinheim